Published in final edited form as:
Mol Pharm. 2010 December 6; 7(6): 2020–2029. doi:10.1021/mp100309y.

Multimodal clinical imaging to longitudinally assess a nanomedical anti-inflammatory treatment in experimental atherosclerosis

Mark E. Lobatto[1], **Zahi A. Fayad**[1,*], **Stephane Silvera**[1], **Esad Vucic**[1], **Claudia Calcagno**[1], **Venkatesh Mani**[1], **Stephen D. Dickson**[1], **Klaas Nicolay**[2], **Manuela Banciu**[3], **Raymond M. Schiffelers**[3], **Josbert M Metselaar**[3], **Louis van Bloois**[3], **Hai-Shan Wu**[4], **John T. Fallon**[4], **James H. Rudd**[1,5], **Valentin Fuster**[6], **Edward A. Fisher**[7], **Gert Storm**[3], and **Willem J.M. Mulder**[1,*]

[1]Translational and Molecular Imaging Institute and Imaging Science Laboratories, Mount Sinai School of Medicine, One Gustave L. Levy Place, New York, New York 10029, USA [2]Biomedical NMR, Department of Biomedical Engineering, Eindhoven University of Technology, PO Box 513, 5600 MB Eindhoven, The Netherlands [3]Department of Pharmaceutics, Utrecht Institute for Pharmaceutical Sciences, Utrecht University, Sorbonnelaan 16, Utrecht 3584 CA, The Netherlands [4]Department of Pathology, Mount Sinai School of Medicine, One Gustave L. Levy Place, New York, New York 10029, USA [5]Division of Cardiovascular Medicine, Addenbrooke's Hospital, ACCI, Box 110, Hills Road, Cambridge CB2 2QQ, UK [6]Mount Sinai Heart, the Zena and Michael A. Wiener Cardiovascular Institute and the Marie-Josée and Henry R. Kravis Center for Cardiovascular Health, Mount Sinai Medical Center, One Gustave L. Levy Place, New York, New York 10029, USA [7]Centro Nacional de Investigaciones Cardiovasculares Carlos III (CNIC), Melchor Fernandez Almagro 3, E-28029 Madrid, Spain [8]Departments of Medicine (Cardiology) and Cell Biology, New York University School of Medicine, New York, NY 10016, USA

Abstract

Atherosclerosis is an inflammatory disease causing great morbidity and mortality in the Western world. To increase the anti-inflammatory action and decrease adverse effects of glucocorticoids (PLP), a nanomedicinal liposomal formulation of this drug (L-PLP) was developed and intravenously applied at a dose of 15 mg/kg PLP to a rabbit model of atherosclerosis. Since atherosclerosis is a systemic disease, emerging imaging modalities for assessing atherosclerotic plaque are being developed. ^{18}F-fluoro-deoxy-glucose positron emission tomography and dynamic contrast enhanced magnetic resonance imaging, methods commonly used in oncology, were applied to longitudinally assess therapeutic efficacy. Significant anti-inflammatory effects were observed as early as 2 days that lasted up to at least 7 days after administration of a single dose of L-PLP. No significant changes were found for the free PLP treated animals. These findings were

[*]**Correspondence**: Willem J. M. Mulder willem.mulder@mountsinai.org, Zahi A. Fayad zahi.fayad@mssm.edu, Translational and Molecular Imaging Institute, Mount Sinai School of Medicine, One Gustave L. Levy Place, Box 1234, New York, NY 10029, Ph. 212-241-7717, Fax. 212-534-2683.

Supporting Information

Supporting Methods
Fig. S1. Schematic of the liposomal nanomedicine.
Fig. S2. Plasma half lives of free PLP and PLP liposomes.
Fig. S3. Liposome concentration in the liver, kidney and spleen.
Fig. S4. PLP concentration in the liver, kidney and spleen.
Fig. S5. CLSM of different regions throughout aortic sections.
Fig. S6. Atherosclerotic plaque histology.

corroborated by immunohistochemical analysis of macrophage density in the vessel wall. In conclusion, this study evaluates a powerful two-pronged strategy for efficient treatment of atherosclerosis that includes nanomedical therapy of atherosclerotic plaques and the application of non-invasive and clinically approved imaging techniques to monitor delivery and therapeutic responses. Importantly, we demonstrate unprecedented rapid anti-inflammatory effects in atherosclerotic lesions after the nanomedical therapy.

Keywords

MRI; FDG-PET; multifunctional liposomes; atherosclerosis; rabbits; glucocorticoids

Introduction

Cardiovascular disease is the leading cause of morbidity and mortality in developed nations (1). Primarily this is caused by atherosclerosis, a systemic disease, characterized by a chronic inflammation of the arterial wall with concomitant vascular lumen lipid deposits (plaques) (2;3). A main challenge is to develop strategies to treat plaque inflammation more effectively. This may be accomplished by developing nanomedical formulations that efficiently target atherosclerotic lesions, accumulate to a much higher extent than free drug formulations and then release the active compound locally at the desired area of interest (4). Additionally, establishing robust endpoints for a given therapy in atherosclerosis is very difficult since the vasculature is a complex and extensive network within the body. Novel imaging strategies have shown great potential in visualizing, quantifying, and characterizing atherosclerosis, and therefore may be used to determine valid endpoints (5–7).

Glucocorticoids are powerful anti-inflammatory agents and one of the drug classes that have been studied in the treatment of inflammation in developing atherosclerotic lesions. An early study with dexamethasone in cholesterol-fed rabbits clearly demonstrated the inhibitory effect on macrophage accumulation in the intima and media of atherosclerotic lesions (8), while Danenberg et al. have shown reduction of in-stent neointimal hyperplasia using liposomal bisphosphonateses (9). As of yet, glucocorticoids have not been seriously considered for clinical treatment of atherosclerosis because they exhibit a poor pharmacokinetic profile. This results in low drug concentrations at sites of intended action, renders them ineffective in treatment, and necessitates high dosages and frequent administration, which causes an array of adverse systemic effects, including diabetes mellitus, osteoporosis and hypertension (10).

To overcome these shortcomings, water-soluble glucocorticoids, such as prednisolone phosphate, can be encapsulated in long-circulating poly(ethylene) glycol (PEG) coated liposomes, which considerably enhances their circulation half-life, thereby increasing their accumulation in inflamed sites (4;11). Liposome-encapsulated prednisolone phosphate (L-PLP) has recently been used in a variety of cancer models (12–15), multiple sclerosis (16) and rheumatoid arthritis (17), where they have been shown to successfully inhibit inflammation and reduce neovascularization.

In the present study we evaluated the therapeutic efficacy of MRI detectable liposomal PLP, schematically depicted in Fig. S1, in a rabbit model of atherosclerosis using a multimodal imaging setup and clinical scanners. The liposomal delivery was visualized by magnetic resonance imaging (MRI). ^{18}F-fluoro-deoxy-glucose positron emission tomography combined with computed tomography (^{18}F-FDG-PET/CT), an imaging method used routinely for the visualization of metastases in cancer patients (18;19), has recently been exploited as an imaging modality for visualizing and quantifying plaque macrophage

inflammation (20–23). Therefore, we applied this imaging method to monitor the effects of the anti-inflammatory nanomedicine in atherosclerotic arteries serially and non-invasively. Inflammation is often accompanied by ongoing neovascularization (angiogenesis), a deleterious process affecting the adventitia in atherosclerosis (24). Dynamic contrast enhanced MRI (DCE-MRI) is an imaging method that allows the investigation of early angiostatic effects in tumors (25;26), but we recently reported the applicability of this technique for atherosclerotic plaque neovascularization as well (27). Since it was shown recently that liposomal glucocorticoids inhibit tumor angiogenesis (12;15), we also applied DCE-MRI of the vessel wall to investigate anti-angiogenic activity non-invasively.

Experimental Section

Animal protocol

Thirty-nine male NZW rabbits (mean age 7 months; Covance) were included in this study. Aortic atherosclerotic plaques were induced in 37 NZW rabbits, through a well established model (43), by a combination of 7 months of high cholesterol diet (4.7% palm oil and 0.3% cholesterol-enriched diet; Research Diet Inc.) and a repeated balloon injury of the aorta (2 weeks and 6 weeks after starting the high cholesterol diet), at seven months mean weight was established at 3.5 ± 0.3 kg. Two non-injured NZW rabbits fed a normal chow diet were used as non-atherosclerotic controls.

Aortic injury was performed from the aortic arch to the iliac bifurcation with a 4F Fogarty embolectomy catheter introduced through the femoral artery. All procedures were performed under general anesthesia by an intramuscular injection of Ketamine (20 mg/kg; Fort Dodge Animal Health), Xylazine (10 mg/kg; Bayer Corp.) and Acepromazine (5 mg/kg: Boehringer Ingelheim). Plaque biology of induced atherosclerotic lesions of the abdominal aorta of rabbits closely resembles atherosclerotic lesions of humans; the diameter is approximately the size of a human coronary artery. All experiments were approved by the Mount Sinai School of Medicine Institute Animal Care and Use Committee.

Liposomal glucocorticoids

Long-circulating liposomes were prepared as described previously (12;17;44). In brief, 51.5 % 1,2-dipalmitoyl-sn-Glycero-3-Phosphocholine (DPPC); 33.3 % cholesterol; 5.0 % 1,2-distearoyl-sn-glycero-3-phosphoethanolamine-N-[methoxy(polyethylene glycol)-2000] (PEG-DSPE); 10 % Gd-DTPA-bis(stearylamide) (Gd-DTPA-BSA); 0.2 % 1,2-dipalmitoyl-sn-glycero-3-phosphoethanolamine-N-(Lissamine Rhodamine B Sulfonyl) (Rhodamine-PE) were dissolved in chloroform: methanol (2:1 vol/vol) in a round-bottom flask. A lipid film was made under reduced pressure on a rotary evaporator and dried under a stream of nitrogen. Liposomes were formed by addition of an aqueous solution of 100 mg/ml prednisolone phosphate disodium salt (Bufa, Uitgeest, The Netherlands). A water-soluble phosphate derivative of prednisolone was used to ensure stable encapsulation in the liposomes. Liposome size was reduced by multiple extrusion steps through polycarbonate membranes (Nuclepore, Pleasanton, Calif., U.S.) with a final pore size of 100 nm. The mean size and zeta potential were determined to be 103 nm and −2 meV, respectively.

MRI

MRI was used to monitor delivery of liposomal PLP into atherosclerotic plaques. Rabbits were sedated with Ketamine/Xylazine/Acepromazine (as above) and imaged supine in a 1.5-Tesla MRI clinical system (Siemens, Sonata, Germany) using high-resolution MR imaging (i.e., pre- and post-contrast, T1-weighted, TR 800 ms, TE 5.60 ms, FOV:120 × 120 mm, 3.00 slice thickness/1.50 spacing, 256 × 256 with 4.0 signal averages). After a pre-treatment scan was performed, liposomal PLP was administered. MR images were acquired pre-

injection, immediately after injection and 2, 7, 14 and 21 days post-injection of the liposomes. Rabbits were positioned to match pre and post-contrast scans by aligning corresponding vertebrae.

DCE-MRI was performed according to a protocol we published recently (27). In short, the change of signal intensity in a region of interest (ROI) including the entire atherosclerotic plaque during the injection of the contrast agent was studied with a custom-made Matlab (The MathWorks, Inc., Natick, MA, USA) program. The area under the signal intensity versus time curve (AUC) for the acquisition of 15 minutes was calculated via the trapezoidal rule of the time series by numerical integration.

PET/CT imaging

PET/CT was used to track changes in plaque inflammation in response to the administration of liposomal PLP. PET/CT scanning was performed on a GE advance LS 16 slice PET/CT scanner. This system has PET and CT components mounted back-to-back, and is mechanically calibrated so that alignment between the two parts is within 2 mm in the transaxial field of view. Rabbits were fasted for 4 hours prior to ^{18}F-FDG injection, with water given ad libitum. They were scanned pre-injection and 2, 7, 14 and 21 days post-injection of the treatment.

The rabbits were imaged under general anesthesia and secured with a Velcro blanket during imaging. They were injected with 1 mCi/Kg ^{18}F-FDG administered over 20 seconds via the marginal ear vein. Imaging started 180 minutes after ^{18}F-FDG injection, which is the optimal time point according to previous studies (21). PET/CT imaging covered the region from the superior mesenteric artery to the aortic bifurcation. The bladder was emptied prior to scanning to allow for a clear view of the distal aorta. Images were acquired in 3D mode with the following parameters: Field of view (FOV) 15.5 cm per bed; single bed position; 10 minutes imaging per bed position. Iterative reconstruction was performed with a 30 cm FOV, giving a reconstructed slice thickness of 4.25 mm. PET/CT images were calibrated to the injected dose of ^{18}F-FDG.

PET/CT images were analyzed on a Xeleris 2.0 workstation (GE, Milwaukee, WI, USA). Arterial ^{18}F-FDG uptake (as a measure of arterial inflammation) in the aorta was measured by drawing a region of interest around the aorta on every slice of the co-registered transaxial PET/CT images. On each image slice, the mean SUV of ^{18}F-FDG in the artery was calculated as the mean pixel activity within the ROI. The SUV is the decay-corrected tissue concentration of ^{18}F-FDG (in kBq/g), corrected for injected ^{18}F-FDG dose and body weight (in kBq/g), and is a well-recognized method for quantification of ^{18}F-FDG-PET data.

Experimental set-up

Rabbits were randomly assigned to receive a single injection of liposomal PLP or free PLP. The drugs were administered to the rabbits through the marginal ear vein at a dose of 15 mg/kg. Figure 1 displays the different scanning and histology time points.

Statistical analysis

Data are presented as the mean ± SD. Statistical analysis was performed using paired t-test for comparisons within groups. Statistical significance was established at $P < 0.05$.

Results

Liposomal PLP exhibits favorable pharmacokinetics and accumulates in atherosclerotic lesions

Liposomal PLP exhibited a dramatically elevated circulation half-life as compared to free PLP (Fig. S2). Importantly, the L-PLP, the PLP and gadolinium labeled liposomes displayed a similar pharmacokinetic profile, indicative of the intactness of the PLP liposomes in circulation. High levels of liposomes were observed in the spleen and liver, 2 days after intravenous administration, which remained the same 7 days after administration (Fig. S3). On the other hand, the initially high PLP levels in these organs at 2 days showed a 4-fold reduction at 7 days post administration (Fig. S4), demonstrating that the PLP are released once the liposomes accumulate in these organs.

Groups of animals that were either treated with liposomal PLP (n=14) or free PLP (n=8) were serially imaged with different imaging techniques according to the overview depicted in Fig. 1. Several animals were randomly sacrificed at different time points to enable *ex vivo* histological and immunofluorescent analyses.

T1-weighted MRI of the abdominal aorta of atherosclerotic New Zealand White (NZW) rabbits was performed to monitor the delivery of gadolinium-labeled liposomal PLP after intravenous administration. Fig. 2A shows an MR image of a rabbit aortic wall before (left) and 2 days after (right) the administration of PLP liposomes. A clear signal intensity increase throughout the entire inflamed vessel wall was observed, indicative of a considerable accumulation of liposomes within the atherosclerotic lesions. The mean signal increase of the vessel wall 2 days after administration was established to be 27 % ± 12.5 %.

To further explore the uptake and localization of liposomes within the inflamed vessel wall we performed liposome determinations as well as near infrared fluorescence (NIRF) imaging on intact aortas and confocal laser scanning microscopy (CLSM) on multiple aortic sections taken from different animals. We measured a mean concentration of 175 and 120 ug liposomes per gram of aortic tissue at 2 and 7 days post intravenous administration, respectively. NIRF imaging showed Cy5.5 labeled liposomes distributed throughout the entire atherosclerotic aorta (Fig. 2B). For CLSM, the liposomes were labeled with rhodamine and could be identified as red fluorescent regions in the aortic sections (Fig. 2C and D). Cell nuclei were stained with DAPI (Fig. 2C, blue), while fluorescently labeled RAM-11 antibodies enabled the identification of macrophages (Fig. 2C, green). In the fused CLSM (Fig. 2D) it was appreciated that liposomes were mainly found to be associated with macrophages. Although in all sections liposomes were found throughout the entire aortic plaque (Fig. S5), the quantity of liposome accumulation was heterogeneously distributed. In Fig. 2E a reconstruction of an entire aortic section is depicted that consists of 35 individually acquired 10× CLSM images. The corresponding MR image is shown in Fig. 2F. The regions that contained a high proportion of rhodamine-labeled liposomes as visualized with CLSM corresponded with hyperintense areas in the aortic wall on MRI (arrows Fig. 2E and F).

Anti-inflammatory effects of liposomal PLP on the atherosclerotic vessel wall were observed by ^{18}F-FDG PET/CT imaging

To evaluate the therapeutic efficacy of the liposomal PLP, 25 atherosclerotic NZW rabbits were imaged using ^{18}F-FDG PET/CT. These scans provide quantifiable information about the level of inflammation present in the abdominal aorta (20).

Prior to the start of the treatment study, the aortas of 6 atherosclerotic rabbits and 2 non-atherosclerotic rabbits were imaged to establish mean standard uptake value (SUV) levels of ^{18}F-FDG in the abdominal aortic wall of both atherosclerotic and non-atherosclerotic

rabbits and to validate the robustness of this imaging technology in the assessment of atherosclerosis related inflammation in rabbits. These measurements resulted in SUV levels of 0.65 ± 0.03 for atherosclerotic rabbits and 0.23 ± 0.03 for non-atherosclerotic rabbits, comparable to values reported by others (28). Several studies by different research groups have revealed a good correlation between macrophage density and SUV levels (28–30). In studies at our laboratory we also found the same high degree of correlation between these two parameters.

In Fig. 3A, coronal CT, PET and fused PET/CT images of the aorta of an atherosclerotic rabbit are shown. Hotspots of ^{18}F-FDG uptake were clearly visible throughout the aorta before treatment with liposomal PLP (top), whilst a reduced ^{18}F-FDG uptake was observed after seven days treatment, demonstrating the efficacy of liposomal PLP. The mean SUV of the different groups, *i.e.* liposomal PLP treated, free (*i.e.* not encapsulated in liposomes) PLP treated, and healthy animals at base level are shown in Figure 3B. Two days and seven days post-treatment, rabbits injected with liposomal PLP showed a significant reduction in SUV (two days $p = 0.0025$, seven days $p = 0.0036$), while for rabbits that were treated with free circulating PLP no significant SUV differences were found (two days $p = 0.56$, seven days $p = 0.41$) at these time points. From day 14 post-treatment SUV levels were not significantly different from baseline level. The relative changes in SUV were determined by [(post-healthy/ (pre-healthy)] and are displayed in Fig. 3C as an extraction of the previous graph. We observed that the relative SUV decreased by 40% for rabbits treated with liposomal PLP compared to rabbits treated with free PLP. To ensure that the decrease in SUV was not the result of gadolinium toxicity, 3 atherosclerotic rabbits were treated with subsequent injections of empty liposomes labeled with gadolinium and free PLP. The SUV levels did not significantly differ at the different time points and were 0.63 ± 0.06 at baseline, and 0.60 ± 0.07 and 0.64 ± s0.07 at day 2 and day 7, respectively (2 days $p = 0.49$, 7 days $p = 0.21$).

DCE-MRI revealed early changes in plaque permeability after liposomal glucocorticoid treatment

A total of 10 rabbits (6 treated with L-PLP and 4 with free PLP) underwent dynamic contrast enhanced MRI (DCE-MRI) before and 2 days after the onset of therapy. This technique requires the acquisition of sequential images before and after the administration of contrast agent (Gd-DTPA, Magnevist); the images obtained during the acquisition can be analyzed calculating the pixel-by-pixel area under the curve (AUC) of the signal intensity versus time. AUC is a parameter that can express the uptake and retention of contrast agent in the region of interest (*i.e.* vessel wall) and correlates with neovascularization of the vasa vasorum in the atherosclerotic vessel wall. Our group recently validated this technique for the detection of neovascularization within atherosclerotic plaque of rabbits (27).

In Fig. 3D, a typical AUC map of the vessel wall before and 2 days after the application L-PLP is shown and clearly demonstrates a decrease in AUC. The mean AUC before and 2 days after onset of therapy revealed a significant reduction from 2278 ± 406 to 1784 ± 449 (A.U.) for L-PLP treated animals, while the AUC for the free PLP treated animals remained the same: 2384 ± 924 before and 2351 ± 488 (A.U.) 2 days after treatment.

Plaque macrophage density determined ex vivo corroborated the in vivo PET imaging data

After the PET scans, aortas were excised and sectioned in segments corresponding to reconstructed PET/CT axial slices. Quantitative immunohistochemistry measurements of macrophages were performed to validate PET findings. With that objective, two animals from each group (healthy, 1 week L-PLP, 1 week free PLP, 3 weeks L-PLP) were sacrificed and macrophage density was quantified. Fig. 4A–C show images of Masson's trichrome (marker of connective tissue) and RAM-11 (marker of macrophage) stained sections with

different treatments/time points. Fig 4D displays the corresponding SUV values determined by in vivo PET imaging. A good correlation (Pearson correlation coefficient r = 0.78) between SUV and macrophage density in corresponding sections was observed (Fig. E). Macrophage density in rabbits treated with liposome-encapsulated PLP was lower than in rabbits treated with free PLP corresponding to findings from the ^{18}F-FDG-PET/CT imaging. No macrophages were detected by immunohistochemistry in the aortic wall of healthy rabbits. Three weeks after treatment with liposome-encapsulated PLP, macrophage density was back to base level (Fig. 4D), similar to findings of the three-week PET/CT scan. Furthermore, we qualitatively assessed monocyte chemoattractant protein-1 (MCP-1) expression in non treated animals and treated animals. MCP-1 monocyte chemoattractant protein-1 (MCP-1) plays a crucial role in the initiation of atherosclerosis and has direct effects that promote inflammation (31) and angiogenesis (32). A decrease in MCP-1 expression was observed (Fig. S6A and B), indicative of a reduction of the afore-mentioned processes. In addition to the MCP-1 staining, endothelial cells were stained to confirm neovascularization in the adventitia of plaque (Fig. S6C).

Discussion

In this study we have shown (a) the potential applicability of long-circulating liposomes as a carrier system for efficient anti-inflammatory/anti-angiogenic drug delivery to atherosclerotic plaques. In addition, we were able to (b) monitor the delivery of these nanomedicines by MRI, which was confirmed using immunofluorescence techniques at (sub)cellular level. In our study, the glucocorticoid prednisolone phosphate (PLP) was encapsulated into long-circulating liposomes. We demonstrated that (c) clinical imaging, i.e. ^{18}F-FDG-PET/CT and DCE-MRI, can be used to monitor the fast therapeutic responses of liposomal PLP. Most importantly, we found that (d) a single injection of liposomal PLP showed a therapeutic effect within 2 days, lasting up to 7 days. Most clinically used anti-inflammatory agents need to be administered for weeks or even months before they are effective (33). To the best of our knowledge, an equally effective and rapid method for reduction of inflammation within atherosclerosis has not been previously reported.

Both *in vivo* and *ex vivo* imaging showed that long-circulating liposomes are highly suitable as a carrier vehicle for drug delivery to atherosclerotic plaques. The therapeutic efficacy of the administration of liposomal PLP is considerably better than free circulating PLP, for which we did not observe significant changes of the inflammatory state of the atherosclerotic lesions. Large quantities of liposomes were found in the atherosclerotic plaque. Atherosclerotic lesions are characterized by angiogenesis and enhanced capillary permeability. The method of targeted delivery and accumulation can be attributed to the "enhanced permeability and retention" (EPR) effect (34): Long-circulating macromolecular materials, such as PEGylated liposomes, extravasate from the bloodstream and accumulate at inflammatory sites where they are retained and act locally. This targeting effect results in an enhanced delivery of drug to the desired site, which enables the use of lower dosages to achieve the same efficacy. Due to the long-circulating properties of the liposomes a higher proportion of the injected dose of the liposome-encapsulated drug as compared to the non-liposomal delivered drug ends up in the plaques. In addition to passive targeting of liposome-encapsulated glucocorticoids, targeted delivery of drugs to sites with enhanced capillary permeability of *e.g.* angiogenic endothelial cells may be accomplished by conjugation of targeting ligands to the liposomal surface. Numerous studies have shown that liposomes can be actively targeted to entities of interest by conjugating targeting molecules to the surface (35). To that end, it is also possible to actively target liposome-encapsulated glucocorticoids to atherosclerotic plaques by e.g. targeting macrophages via the macrophage scavenger receptor (36), neovessels via $\alpha_v\beta_3$-integrin (37;38) or any other target of choice that is upregulated in atherosclerotic lesions (6). Nevertheless, "simple" long circulating

liposomes without targeting ligands are very attractive and even preferred for a number of reasons. They are easier to synthesize, less expensive, more generally applicable, generate less immunoresponse, and most importantly can easier be applied to humans. This has led to the approval and clinical application of a variety of liposomal drugs in the field of oncology (35).

Liposomal PLP was tracked in vivo by high-resolution MRI showing heterogeneous signal enhancement throughout the entire abdominal aorta. Inclusion of amphiphilic gadolinium chelates in the liposomes allowed their visualization in the aortic vessel wall. In addition to paramagnetic labels, other labels may be used to monitor the delivery of liposomes. For instance, it is possible to co-encapsulate liposomes with a radioactive marker to enable detection by PET. In a study investigating anti-inflammatory effects in a rat model of rheumatoid arthritis, liposome-encapsulated glucocorticoids were detected by scintigraphic imaging (17). Since no therapeutic effect can be ascribed to the labels, they can be omitted, which would be essential for human application. In fact, liposomal PLP similar to the liposomes used in our study, without inclusion of gadolinium and fluorescent labels, are currently being evaluated in patients with active rheumatoid arthritis (clinicaltrials.gov identifier: NCT00241982). Studies in atherosclerotic patients are needed to prove the significance of the findings reported in the current study.

In previous studies, ^{18}F-FDG PET/CT has shown to be an effective imaging method to monitor therapeutic effects of anti-inflammatory drugs and risk factor modification in atherosclerosis (28;39). In our study we demonstrated that ^{18}F-FDG PET/CT could be effectively and non-invasively applied to determine the effects of liposomal glucocorticoids. The advantage of PET/CT for monitoring the effect of drugs is that it is a sensitive and robust technique that is used on a regular basis in clinical practice, which facilitates the translation of the presented drug targeting technology to patients. Also, in recent studies from our group, Rudd *et al.* show that ^{18}F-FDG PET/CT of atherosclerotic plaque inflammation is highly reproducible within studies and has high inter- and intra-observer agreement, further acknowledging ^{18}F-FDG-PET as a noninvasive plaque imaging technique (20;40).

Ogawa et al. showed that probucol, an anti-oxidant drug, has a therapeutic effect on rabbit atherosclerotic lesions after three months (28). In our study we have shown that a single injection of liposome-encapsulated glucocorticoids has a similar therapeutic effect within 2 days, lasting up to 7 weeks, before returning to baseline after 2 weeks. This demonstrates that liposome-encapsulated glucocorticoids may be very potent anti-inflammatory drugs not only efficient in *e.g.* rheumatoid arthritis and cancer but also in the treatment of atherosclerosis by reducing the amount of macrophages in a short time period without systemic toxicity as seen with free circulating glucocorticoid administration (10). This greatly enhances benefit-risk ratios and is a step forward toward a clinically viable treatment for advanced atherosclerotic lesions. The exact pathway is not known, but it is believed that high concentrations of PLP shows non-genomic effects in addition to their genomic effects, causing a reduction of macrophage infiltration (41). Further effects of liposome-encapsulated glucocorticoids must be researched by examining plaque biology and different inflammatory markers. By changing the treatment schedule or intensity, for instance, injecting multiple doses over a prolonged period of time or combining the presented treatment with lipid lowering therapies, long-term regression may be achieved. Statins can reduce plasma cholesterol and have anti-inflammatory effects, but they do not always lead to stabilization of vulnerable or high-risk plaques. Combination with liposome-encapsulated glucocorticoids may lead to a powerful one-two combination, ultimately achieving long-term regression of atherosclerosis.

A combined approach of MR imaging and drug targeting has been performed previously in atherosclerosis. Winter *et al.* published results on a combinatory approach of MR molecular imaging and drug targeting of atherosclerosis using αvβ3-specific nanoparticles (42). They used these nanoparticles to target the aortic vessel wall of atherosclerotic rabbits. For therapeutic purposes, they included fumagillin in the lipid monolayer of the nanoparticles and observed an anti-angiogenic effect with MRI that was confirmed histologically.

In this study we obtained preliminary results about early anti-angiogenic effects on the atherosclerotic lesions with this liposomal compound using DCE-MRI. Recently, it has been shown using molecular biological techniques that liposome-encapsulated PLP exhibits anti-angiogenic effects in cancer (15). This phenomenon should also contribute to halting progression of atherosclerosis in addition to the anti-inflammatory effects studied in greater detail here.

In conclusion, this study demonstrates a novel anti-inflammatory treatment for advanced atherosclerotic lesions monitored by non-invasive multimodality imaging. Pronounced atherosclerotic lesions in a rabbit model, closely mimicking human lesions, showed a significant and unprecedented rapid decrease in inflammation by a single injection of liposome-encapsulated glucocorticoids. This treatment can be tracked and monitored non-invasively and can be used to achieve reduction of inflammation in atherosclerotic lesions within a short time period with minimal systemic toxicity.

Supplementary Material

Refer to Web version on PubMed Central for supplementary material.

Acknowledgments

Partial support was provided by: NIH/NHLBI R01 HL71021, NIH/ NHLBI R01 HL78667 (ZAF) and the Peter Jay Sharp Foundation (WJMM). We gratefully acknowledge the assistance of Suzana Sata, Laura Tessell and Ash Rafique from the Mount Sinai Medical Center for their support with the PET acquisitions. We also acknowledge the support of Drs. Burton Drayer and Josef Machac from the Department of Radiology at Mount Sinai School of Medicine. Confocal microscopy was performed at the MSSM–Microscopy Shared Resource Facility and supported by NIH–National Cancer Institute Grant 5R24 CA095823-04, National Science Foundation Grant DBI- 9724504, and NIH Grant 1 S10 RR0 9145-01.

References

1. Sanz J, Moreno PR, Fuster V. The year in atherothrombosis. J.Am.Coll.Cardiol. 2008; 51:944–955. [PubMed: 18308164]
2. Fuster V, Moreno PR, Fayad ZA, Corti R, Badimon JJ. Atherothrombosis and high-risk plaque: part I: evolving concepts. J.Am.Coll.Cardiol. 2005; 46:937–954. [PubMed: 16168274]
3. Ross R. Atherosclerosis--an inflammatory disease. N.Engl.J.Med. 1999; 340:115–126. [PubMed: 9887164]
4. Chono S, Tauchi Y, Deguchi Y, Morimoto K. Efficient drug delivery to atherosclerotic lesions and the antiatherosclerotic effect by dexamethasone incorporated into liposomes in atherogenic mice. J Drug Target. 2005; 13:267–276. [PubMed: 16051539]
5. Lindsay AC, Choudhury RP. Form to function: current and future roles for atherosclerosis imaging in drug development. Nat.Rev.Drug Discov. 2008; 7:517–529. [PubMed: 18483481]
6. Choudhury RP, Fuster V, Fayad ZA. Molecular, cellular and functional imaging of atherothrombosis. Nat.Rev.Drug Discov. 2004; 3:913–925. [PubMed: 15520814]
7. Sanz J, Fayad ZA. Imaging of atherosclerotic cardiovascular disease. Nature. 2008; 451:953–957. [PubMed: 18288186]

8. Poon M, Gertz SD, Fallon JT, Wiegman P, Berman JW, Sarembock IJ, Taubman MB. Dexamethasone inhibits macrophage accumulation after balloon arterial injury in cholesterol fed rabbits. Atherosclerosis. 2001; 155:371–380. [PubMed: 11254907]
9. Danenberg HD, Golomb G, Groothuis A, Gao J, Epstein H, Swaminathan RV, Seifert P, Edelman ER. Liposomal alendronate inhibits systemic innate immunity and reduces in-stent neointimal hyperplasia in rabbits. Circulation. 2003; 108:2798–2804. [PubMed: 14610008]
10. Czock D, Keller F, Rasche FM, Haussler U. Pharmacokinetics and pharmacodynamics of systemically administered glucocorticoids. Clin.Pharmacokinet. 2005; 44:61–98. [PubMed: 15634032]
11. Metselaar JM, Storm G. Liposomes in the treatment of inflammatory disorders. Expert.Opin.Drug Deliv. 2005; 2:465–476. [PubMed: 16296768]
12. Banciu M, Schiffelers RM, Fens MH, Metselaar JM, Storm G. Anti-angiogenic effects of liposomal prednisolone phosphate on B16 melanoma in mice. J.Control Release. 2006; 113:1–8. [PubMed: 16707187]
13. Banciu M, Metselaar JM, Schiffelers RM, Storm G. Liposomal glucocorticoids as tumor-targeted anti-angiogenic nanomedicine in B16 melanoma-bearing mice. J.Steroid Biochem.Mol.Biol. 2008; 111:101–110. [PubMed: 18602825]
14. Banciu M, Fens MH, Storm G, Schiffelers RM. Antitumor activity and tumor localization of liposomal glucocorticoids in B16 melanoma-bearing mice. J.Control Release. 2008; 127:131–136. [PubMed: 18291548]
15. Banciu M, Metselaar JM, Schiffelers RM, Storm G. Antitumor activity of liposomal prednisolone phosphate depends on the presence of functional tumor-associated macrophages in tumor tissue. Neoplasia. 2008; 10:108–117. [PubMed: 18283332]
16. Schmidt J, Metselaar JM, Wauben MH, Toyka KV, Storm G, Gold R. Drug targeting by long-circulating liposomal glucocorticosteroids increases therapeutic efficacy in a model of multiple sclerosis. Brain. 2003; 126:1895–1904. [PubMed: 12805101]
17. Metselaar JM, Wauben MH, Wagenaar-Hilbers JP, Boerman OC, Storm G. Complete remission of experimental arthritis by joint targeting of glucocorticoids with long-circulating liposomes. Arthritis Rheum. 2003; 48:2059–2066. [PubMed: 12847701]
18. Delbeke D. Oncological applications of FDG PET imaging. J.Nucl.Med. 1999; 40:1706–1715. [PubMed: 10520713]
19. Delbeke D. Oncological applications of FDG PET imaging: brain tumors, colorectal cancer, lymphoma and melanoma. J.Nucl.Med. 1999; 40:591–603. [PubMed: 10210218]
20. Rudd JH, Myers KS, Bansilal S, Machac J, Pinto CA, Tong C, Rafique A, Hargeaves R, Farkouh M, Fuster V, et al. Atherosclerosis inflammation imaging with 18F-FDG PET: carotid, iliac, and femoral uptake reproducibility, quantification methods, and recommendations. J.Nucl.Med. 2008; 49:871–878. [PubMed: 18483100]
21. Rudd JH, Warburton EA, Fryer TD, Jones HA, Clark JC, Antoun N, Johnstrom P, Davenport AP, Kirkpatrick PJ, Arch BN, et al. Imaging atherosclerotic plaque inflammation with [18F]-fluorodeoxyglucose positron emission tomography. Circulation. 2002; 105:2708–2711. [PubMed: 12057982]
22. Tawakol A, Migrino RQ, Bashian GG, Bedri S, Vermylen D, Cury RC, Yates D, LaMuraglia GM, Furie K, Houser S, et al. In vivo 18F-fluorodeoxyglucose positron emission tomography imaging provides a noninvasive measure of carotid plaque inflammation in patients. J.Am.Coll.Cardiol. 2006; 48:1818–1824. [PubMed: 17084256]
23. Tawakol A, Migrino RQ, Hoffmann U, Abbara S, Houser S, Gewirtz H, Muller JE, Brady TJ, Fischman AJ. Noninvasive in vivo measurement of vascular inflammation with F-18 fluorodeoxyglucose positron emission tomography. J.Nucl.Cardiol. 2005; 12:294–301. [PubMed: 15944534]
24. Moreno PR, Purushothaman KR, Sirol M, Levy AP, Fuster V. Neovascularization in human atherosclerosis. Circulation. 2006; 113:2245–2252. [PubMed: 16684874]
25. Padhani AR, Husband JE. Dynamic contrast-enhanced MRI studies in oncology with an emphasis on quantification, validation and human studies. Clin.Radiol. 2001; 56:607–620. [PubMed: 11467863]

26. Padhani AR. Dynamic contrast-enhanced MRI in clinical oncology: current status and future directions. J.Magn Reson.Imaging. 2002; 16:407–422. [PubMed: 12353256]
27. Calcagno C, Cornily JC, Hyafil F, Rudd JH, Briley-Saebo KC, Mani V, Goldschlager G, Machac J, Fuster V, Fayad ZA. Detection of neovessels in atherosclerotic plaques of rabbits using dynamic contrast enhanced MRI and 18F-FDG PET. Arterioscler.Thromb.Vasc.Biol. 2008; 28:1311–1317. [PubMed: 18467641]
28. Ogawa M, Magata Y, Kato T, Hatano K, Ishino S, Mukai T, Shiomi M, Ito K, Saji H. Application of 18F-FDG PET for monitoring the therapeutic effect of antiinflammatory drugs on stabilization of vulnerable atherosclerotic plaques. J.Nucl.Med. 2006; 47:1845–1850. [PubMed: 17079818]
29. Ogawa M, Ishino S, Mukai T, Asano D, Teramoto N, Watabe H, Kudomi N, Shiomi M, Magata Y, Iida H, et al. (18)F-FDG accumulation in atherosclerotic plaques: immunohistochemical and PET imaging study. J.Nucl.Med. 2004; 45:1245–1250. [PubMed: 15235073]
30. Zhang Z, Machac J, Helft G, Worthley SG, Tang C, Zaman AG, Rodriguez OJ, Buchsbaum MS, Fuster V, Badimon JJ. Non-invasive imaging of atherosclerotic plaque macrophage in a rabbit model with F-18 FDG PET: a histopathological correlation. BMC.Nucl.Med. 2006; 6:3. [PubMed: 16725052]
31. Gu L, Okada Y, Clinton SK, Gerard C, Sukhova GK, Libby P, Rollins BJ. Absence of monocyte chemoattractant protein-1 reduces atherosclerosis in low density lipoprotein receptor-deficient mice. Mol.Cell. 1998; 2:275–281. [PubMed: 9734366]
32. Salcedo R, Ponce ML, Young HA, Wasserman K, Ward JM, Kleinman HK, Oppenheim JJ, Murphy WJ. Human endothelial cells express CCR2 and respond to MCP-1: direct role of MCP-1 in angiogenesis and tumor progression. Blood. 2000; 96:34–40. [PubMed: 10891427]
33. Ogawara K, Kuldo JM, Oosterhuis K, Kroesen BJ, Rots MG, Trautwein C, Kimura T, Haisma HJ, Molema G. Functional inhibition of NF-kappaB signal transduction in alphavbeta3 integrin expressing endothelial cells by using RGD-PEG-modified adenovirus with a mutant IkappaB gene. Arthritis Res.Ther. 2006; 8:R32. [PubMed: 16803639]
34. Iyer AK, Khaled G, Fang J, Maeda H. Exploiting the enhanced permeability and retention effect for tumor targeting. Drug Discov.Today. 2006; 11:812–818. [PubMed: 16935749]
35. Torchilin VP. Recent advances with liposomes as pharmaceutical carriers. Nat.Rev.Drug Discov. 2005; 4:145–160. [PubMed: 15688077]
36. Amirbekian V, Lipinski MJ, Briley-Saebo KC, Amirbekian S, Aguinaldo JG, Weinreb DB, Vucic E, Frias JC, Hyafil F, Mani V, et al. Detecting and assessing macrophages in vivo to evaluate atherosclerosis noninvasively using molecular MRI. Proc.Natl.Acad.Sci.U.S.A. 2007; 104:961–966. [PubMed: 17215360]
37. Mulder WJ, Strijkers GJ, Habets JW, Bleeker EJ, van der Schaft DW, Storm G, Koning GA, Griffioen AW, Nicolay K. MR molecular imaging and fluorescence microscopy for identification of activated tumor endothelium using a bimodal lipidic nanoparticle. FASEB J. 2005; 19:2008–2010. [PubMed: 16204353]
38. Winter PM, Morawski AM, Caruthers SD, Fuhrhop RW, Zhang H, Williams TA, Allen JS, Lacy EK, Robertson JD, Lanza GM, et al. Molecular imaging of angiogenesis in early-stage atherosclerosis with alpha(v)beta3-integrin-targeted nanoparticles. Circulation. 2003; 108:2270–2274. [PubMed: 14557370]
39. Tahara N, Kai H, Ishibashi M, Nakaura H, Kaida H, Baba K, Hayabuchi N, Imaizumi T. Simvastatin attenuates plaque inflammation: evaluation by fluorodeoxyglucose positron emission tomography. J.Am.Coll.Cardiol. 2006; 48:1825–1831. [PubMed: 17084257]
40. Rudd JH, Myers KS, Bansilal S, Machac J, Rafique A, Farkouh M, Fuster V, Fayad ZA. (18)Fluorodeoxyglucose positron emission tomography imaging of atherosclerotic plaque inflammation is highly reproducible: implications for atherosclerosis therapy trials. J.Am.Coll.Cardiol. 2007; 50:892–896. [PubMed: 17719477]
41. Schiffelers RM, Banciu M, Metselaar JM, Storm G. Therapeutic application of long-circulating liposomal glucocorticoids in auto-immune diseases and cancer. J.Liposome Res. 2006; 16:185–194. [PubMed: 16952873]
42. Winter PM, Morawski AM, Caruthers SD, Harris TD, Fuhrhop RW, Zhang HY, Allen JS, Lacy EK, Williams TA, Wickline SA, et al. Antiangiogenic therapy of early atherosclerosis with

paramagnetic alpha(v)beta(3)-integrin-targeted fumagillin nanoparticles. Journal of the American College of Cardiology. 2004; 43:322A–323A.

43. Hyafil F, Cornily JC, Feig JE, Gordon R, Vucic E, Amirbekian V, Fisher EA, Fuster V, Feldman LJ, Fayad ZA. Noninvasive detection of macrophages using a nanoparticulate contrast agent for computed tomography. Nat.Med. 2007; 13:636–641. [PubMed: 17417649]
44. Mulder WJ, Strijkers GJ, Griffioen AW, van Bloois L, Molema G, Storm G, Koning GA, Nicolay K. A liposomal system for contrast-enhanced magnetic resonance imaging of molecular targets. Bioconjug.Chem. 2004; 15:799–806. [PubMed: 15264867]

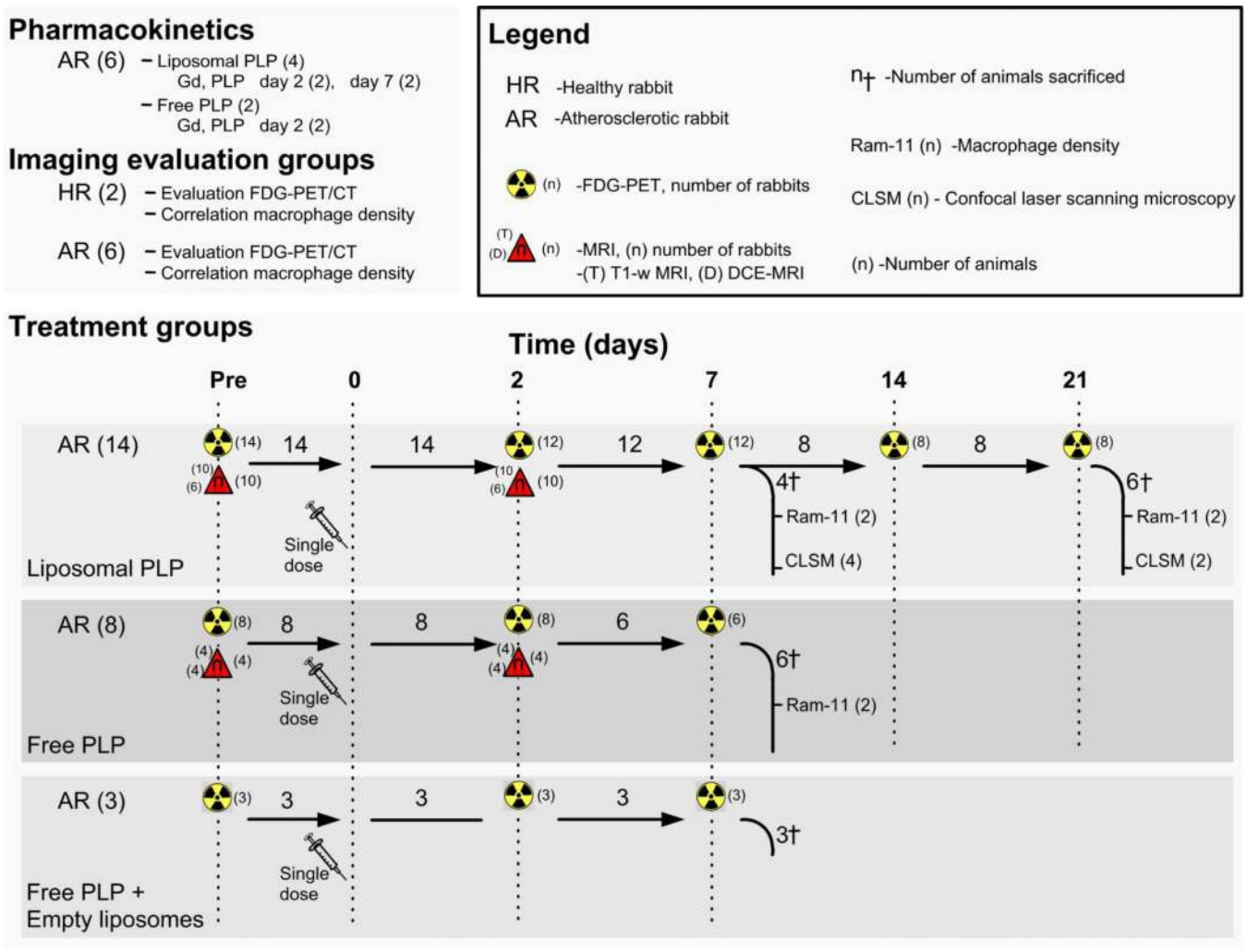

Fig. 1. Pharmacokinetics, imaging and treatment scheme

The organ distribution and pharmacokinetic profile of liposomal PLP and free PLP were evaluated in 6 atherosclerotic rabbits. Two healthy rabbits and 6 atherosclerotic rabbits (top, left) were used to quantify the mean uptake values of ^{18}F-FDG using PET/CT imaging. The treatment groups consisted of a group of 14 atherosclerotic rabbits that received a single dose of liposomal PLP and a group of 8 atherosclerotic rabbits that received a single dose of free PLP (bottom). All animals underwent baseline scanning, multimodality imaging was performed at different time points post treatment to visualize liposome accumulation in the vessel wall and to quantify inflammation of the abdominal aorta. Immunofluorescence and histological analyses were performed on randomly selected animals at the indicated time points.

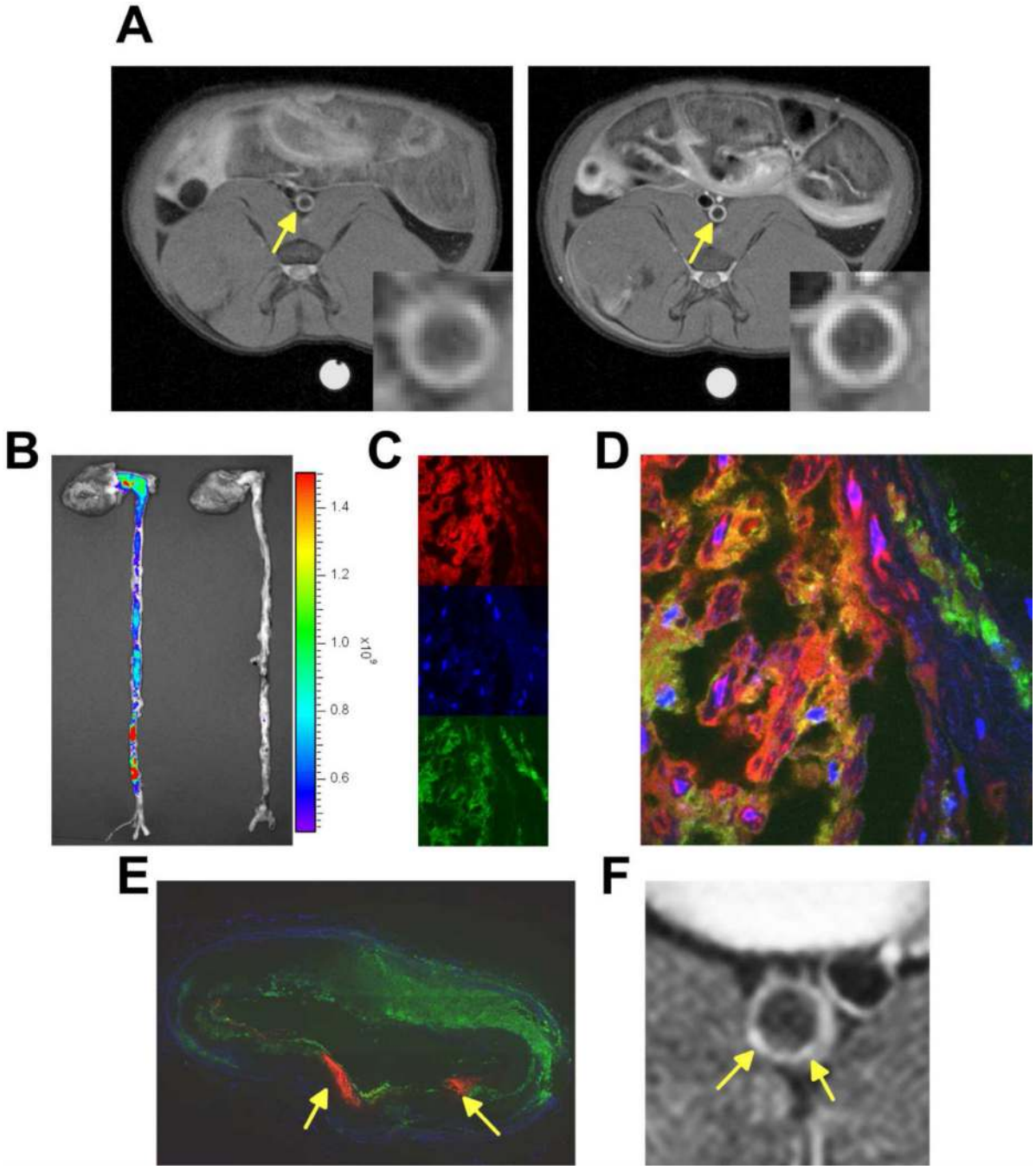

Fig. 2. Images of delivery and localization of liposomal PLP by MRI and confocal laser scanning microscopy

(A) In vivo MRI of the abdominal aorta before (left) and two days after (right) the administration of liposomes. A marked signal intensity increase was observed throughout the atherosclerotic lesion. (B) NIRF images of an atherosclerotic aorta excised from a rabbit injected with liposomes (left) and untreated aorta (right). The color bar represents photon count. (C) CLSM of liposomes (red), cell nuclei (blue), and macrophages. (D) A high degree of co-localization of liposomes with macrophages was observed. (E) Although liposomes were found throughout the entire lesion areas, a vessel wall reconstruction of multiple CLSM images revealed heterogeneous accumulation of liposomes. F) The corresponding

MRI slice of the histological section depicted in (E) revealed a similar heterogeneous distribution.

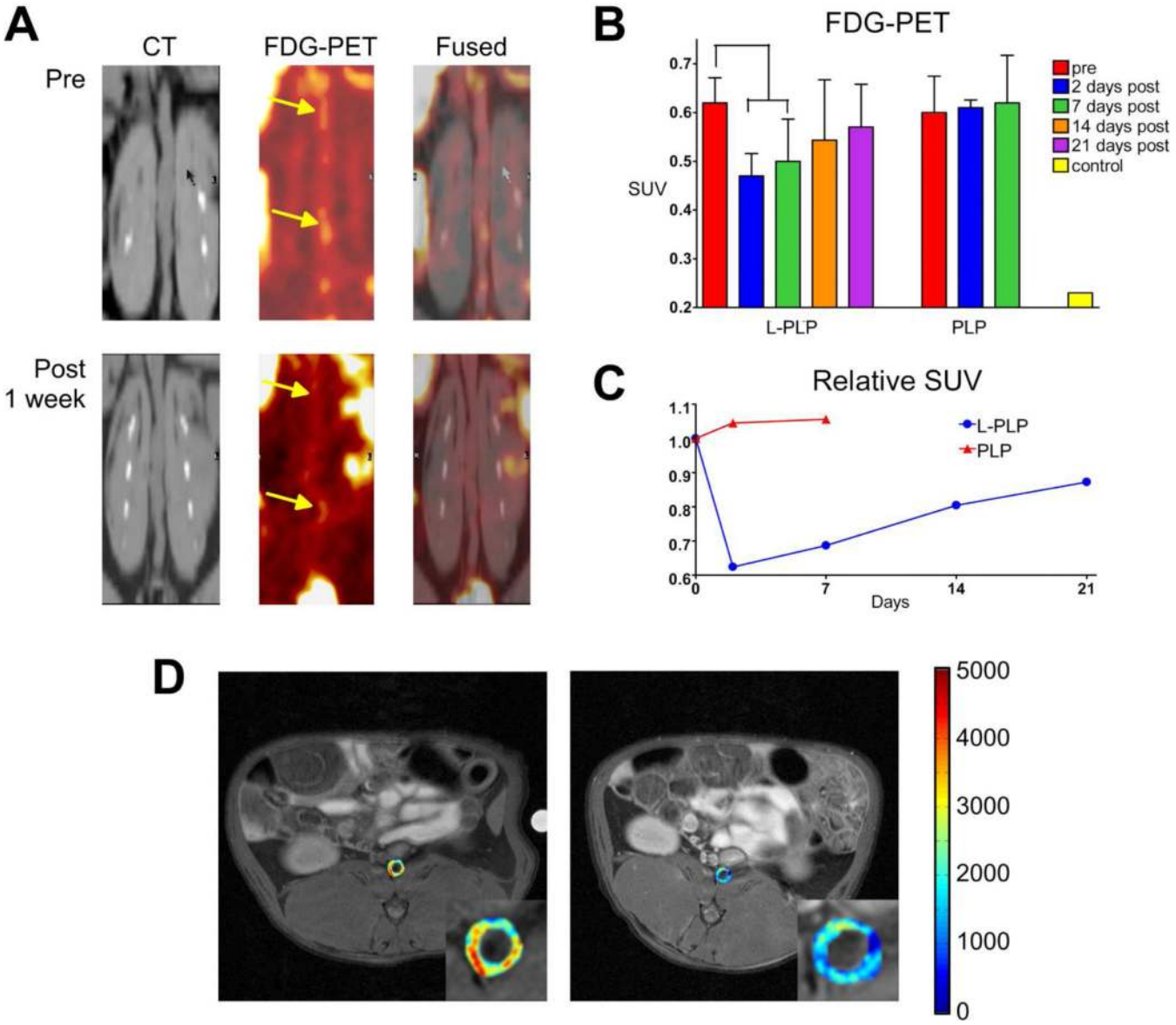

Fig. 3. Non-invasive imaging of therapeutic effects as determined by ^{18}F-FDG-PET and DCE-MRI

(A) A representative coronal CT, ^{18}F-FDG-PET, and fused imaging slice throughout the abdominal aorta of an atherosclerotic rabbit before and 1 week post administration of liposomal PLP. (B) The mean SUV for the different time points pre and post-injection of liposomal PLP and free PLP are given. (C) Relative changes in SUV for animals treated with liposomal and free PLP. (D) Overlays on anatomical images of AUC maps obtained with DCE-MRI before (left) and two days post (right) treatment with liposomal PLP.

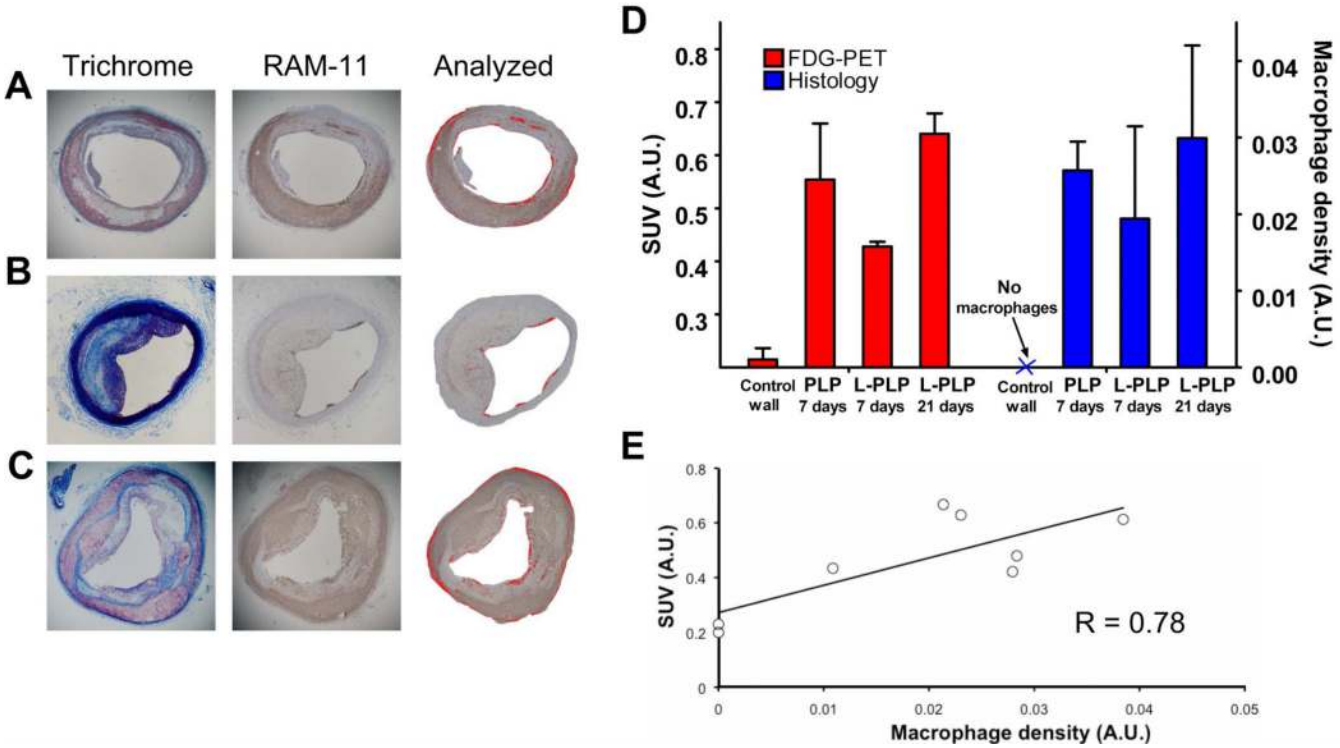

Fig. 4. Correlation between histology and non-invasive ^{18}F-FDG-PET imaging

Representative histological slices of aortic sections stained with Masson's trichrome and stained for macrophages with RAM-11. (A) Section from a free PLP treated animal, 7 days after intravenous administration. (B) Macrophage density is significantly reduced 7 days post-treatment with liposomal PLP and was (C) back to baseline after 21 days. (D) The mean SUVs (left) for the rabbits that underwent histological quantification of macrophage density (right). (E) Correlation between macrophage density determined histologically and SUV determined by non-invasive imaging (FDG-PET).